Published in final edited form as:
Magn Reson Med. 2015 February ; 73(2): 646–654. doi:10.1002/mrm.25190.

Dynamic inversion time for improved 3D late gadolinium enhancement imaging in patients with atrial fibrillation

Jennifer Keegan[1], **Peter D Gatehouse**[1], **Shouvik Haldar**[2], **Ricardo Wage**[3], **Sonya V Babu-Narayan**[1,4], and **David N Firmin**[1,4]

[1]Cardiovascular Biomedical Research Unit, Royal Brompton and Harefield NHS Trust, London

[2]Department of Cardiology, Royal Brompton and Harefield NHS Trust, London

[3]Cardiovascular Magnetic Resonance Unit, Royal Brompton and Harefield NHS Trust, London

[4]Imperial College of Science Technology and Medicine, London.

Abstract

Purpose—High resolution 3D late gadolinium enhancement (LGE) imaging is performed with single R-wave gating to minimise lengthy acquisition durations. In patients with atrial fibrillation (AF), heart rate variability results in variable magnetisation recovery between sequence repeats and image quality is often poor. In this study, we implemented and tested a dynamic inversion time scheme designed to reduce sequence sensitivity to heart rate variations.

Methods—An inversion-prepared 3D segmented gradient echo sequence was modified so that the inversion time (TI) varied automatically from beat-to-beat (dynamic-TI) based on the time since the last sequence repeat. 3D LGE acquisitions were performed in 17 patients prior to RF ablation of persistent AF both with and without dynamic-TI. Qualitative image quality scores, blood signal-to-ghosting ratios (SGRs) and blood-myocardium contrast-to-ghosting ratios (CGRs) were compared.

Results—Image quality scores were higher with dynamic-TI than without (2.2 +/− 0.9 versus 1.8 +/− 1.1, p = 0.008) as were blood-myocardium CGRs (13.8 +/− 7.6 versus 8.3 +/− 6.1, p = 0.003) and blood SGRs (19.6 +/− 8.5 versus 13.1 +/− 8.0, p = 0.003).

Conclusions—The dynamic-TI algorithm improves image quality of 3D LGE imaging in this difficult patient population by reducing the sequence sensitivity to RR interval variations.

Keywords

late gadolinium enhancement imaging; 3D; arrhythmia

Introduction

Atrial fibrillation (AF) is the most prevalent form of cardiac rhythm disturbance and is associated with increased rates of stroke, heart failure and death (1). Radiofrequency

Address for correspondence: Dr Jennifer Keegan Cardiovascular Magnetic Resonance Royal Brompton Hospital Sydney Street, London SW3 6NP j.keegan@rbht.nhs.uk Tel: 020 7351 8800 Fax: 020 7351 8816.

Europe PMC Funders Author Manuscripts

ablation is a common treatment (2), the aim being to electrically isolate the pulmonary veins which are a frequent source of ectopic beats (3). The procedure carries a risk of major complication (4) and repeat procedures are often necessary, with a recent meta-analysis (4) reporting a success rate for single-procedure catheter ablation of persistent AF of 50.8% at 1 year and 41.6% at 3 years. The corresponding success rates for paroxysmal AF are 68.6% and 61.1%.

There has recently been considerable interest in 3D late gadolinium enhancement (LGE) imaging in the AF population where scarring following radio frequency ablation has been demonstrated (5,6) and quantified (7-9). In addition, its spatial distribution and extent has been shown to be related to the likelihood of recurrence (10) and it may be helpful in directing the electrophysiologist to regions of incomplete scarring in repeat procedures (11). As well as assessing the left atrium post ablation, the degree of late enhancement in pre-ablation studies has been shown to be related to the risk of stroke (12) and is associated with sinus node dysfunction requiring pacemaker implantation (13). Pre-ablation LGE is also important for stratifying patients in order to identify predictors of successful ablation (14,15) and for tailoring the ablation strategy to the individual patient (16).

Conventional breath-hold 2D LGE imaging (17) is acquired with alternate R-wave gating which allows almost complete recovery of the longitudinal magnetisation from one sequence repeat to the next and which is consequently relatively robust to changes in the RR interval throughout the acquisition. This is demonstrated in Figure 1(a) where the longitudinal magnetisation is plotted over time for alternate R-wave gated acquisitions in a subject with a variable RR interval. High resolution 3D LGE imaging is performed during free-breathing using diaphragmatic navigators to restrict the respiratory motion and in order to reduce the otherwise lengthy acquisition durations, studies are gated on consecutive cardiac cycles (single R-wave gating). With single R-wave gating, however, the longitudinal magnetisation recovery following inversion preparation between sequence repeats is incomplete (Figure 1(b)) and, in the presence of RR interval variations, it can be highly variable. This can result in ghosting and poor nulling of normal myocardium which is exacerbated by missed cardiac triggers which become more likely when the RR interval changes. A missed trigger results when an R-wave occurs during the acquisition of a data segment (due to a short RR interval) and delays the acquisition of the next data segment until the next R-wave trigger is received. In the AF population then, image quality is frequently poor (18) and the percentage of non-diagnostic scans can be high with values of 31% (7), 13% (8), 41% (10) and 15% (14) having been reported recently. In one study, pre-ablation patients were frequently cardioverted to restore normal sinus rhythm before LGE acquisition (7), but this is not always a practical option clinically. A saturation/inversion recovery sequence (19) has recently been introduced and phantom experiments and simulations have shown that this reduces ghosting artefacts and results in improved nulling, albeit at the expense of some loss in contrast-to-noise ratio. However, while results in a single patient with AF were promising, the technique has not yet been systematically assessed *in vivo*.

In this manuscript, we suggest a different approach to reducing the problems associated with heart rate variability. Real-time adaptation of the inversion time (dynamic-TI) in response to changes in RR interval has been shown to improve image quality in double inversion (dark

blood) prepared turbo spin echo imaging for T2 assessment in thalassemia patients (20). We propose that such a technique could reduce changes in the longitudinal magnetisation throughout a 3D LGE acquisition and hence reduce sensitivity to arrhythmia in patients with AF. To this end, we have developed a dynamic-TI inversion prepared sequence and have acquired 3D LGE data both with and without the dynamic-TI algorithm in seventeen patients with persistent AF prior to RF ablation.

Methods

An inversion-prepared segmented 3D gradient echo sequence was modified to allow real-time adaptation of the inversion time, based on the time since the last sequence repeat. The gating delay was also modified on a beat-to-beat basis so that data was always acquired at the same time in each cardiac cycle. The dynamic-TI algorithm calculated the inversion time required to null normal myocardium for sequence repeat n (TI_n) as (21):

$$Tl_n = T1_{myo}{}^{*}\left(\log_e(2) - \log_e\left(1+\exp\left(-TR_{n-1}/T1_{myo}\right)\right)\right) \quad (1)$$

where: $T1_{myo}$ is the estimated T1 of normal myocardium (as discussed below) and TR_{n-1} is the time since the last sequence repeat

The reference inversion time required to null normal myocardium in a conventional breath-hold 2D inversion prepared LGE acquisition (TI_{ref}) and the time between sequence repeats for that TI_{ref} acquisition (generally 2 × R-R intervals but increased to 3 or 4 × RR intervals for very fast heart rates) were included in the sequence protocol parameters. The time between sequence repeats was estimated from a visual display of the ECG trace. The myocardial T1 ($T1_{myo}$) was initially estimated as TI_{ref}/0.693 and was then iteratively adjusted to take into account the sequence repeat time at which the TI_{ref} was determined (2 × R-R interval). A checkbox was included which enabled the selection or de-selection of the dynamic-TI algorithm. If the dynamic-TI checkbox was not selected (ie the acquisition was to be performed with a fixed TI), a target sequence repeat time interval for which the fixed TI was to be calculated was also input. The sequence was also modified to store the sequence repeat time intervals through the acquisition in a text file for subsequent analysis.

Phantom Studies

The efficacy the dynamic-TI algorithm was demonstrated in acquisitions of a phantom consisting of three bottles with T1s representing normal myocardium (490 ms), blood pool (420 ms) and a shorter T1 tissue (360 ms) following gadolinium administration. A conventional 2D breath-hold inversion-prepared LGE acquisition (with a simulated RR interval of 1000 ms and alternate R-wave gating) with centric phase encoding was performed to determine the inversion time required to null the bottle representing normal myocardium (TI_{ref}). 3D LGE acquisitions showing cross-sections of these bottles were then performed using an inversion-prepared segmented gradient echo sequence (TE = 2.3 ms, TR = 5.2 ms) as follows: 18 slices at 1.5mm × 1.5mm × 4mm, reconstructed to 36 slices at 0.7mm × 0.7mm × 2mm, through-plane over-sampling 12.5%, field of view 380 mm × 380 mm × 128 – 144 mm, generalised autocalibrating partially parallel acquisition (GRAPPA (22)) x2, 24 lines per cardiac cycle with an acquisition window of 125 ms, single R-wave

gating, centric kz and centric ky ordering, flip angle 20°. The inversion time for all 3D acquisitions was determined on the scanner by equation (1), the user inputting the TI_{ref} determined in the 2D acquisition, the sequence repeat time interval at which this TI_{ref} was obtained (2 × simulated RR interval = 2000 ms) and selecting or de-selecting the dynamic-TI checkbox. If acquisitions were peformed without dynamic-TI, a target sequence repeat time interval was also input for calculation of a fixed TI. The following acquisitions were performed: (1) fixed simulated RR interval of 1000 ms, alternate R-wave gating, TI to null simulated myocardium (TI_{ref}), (2) fixed simulated RR interval of 1000 ms, single R-wave gating, fixed TI calculated from equation (1) for a target sequence repeat time of 1000 ms, (3) simulated RR interval varying randomly from 730 ms – 1300 ms, single R-wave gating, fixed TI calculated from equation (1) for a target sequence repeat time of 1000 ms (4) simulated RR interval varying randomly from 730 ms – 1300 ms, single R-wave gating, TI calculated dynamically from beat-to-beat, (5) as for (3) but with frequent missed cardiac triggers, (6) as for (4) but with frequent missed cardiac triggers. Acquisitions (3) – (6) were each repeated five times and the simulated blood-myocardium contrast-to-ghosting ratio (CGR) and simulated enhanced tissue-myocardium CGR determined in each case.

Simulation Study

For 16 sequence repeat time intervals, Bloch equation simulations were performed to determine the longitudinal magnetisation (Mz) of normal myocardium (T1 490 ms), blood (T1 420 ms) and a shorter T1 tissue (T1 360 ms) prior to the acquisition of the most centric phase encode line in each data segment. Sequence repeat times (TR = 5.2 ms), number of phase encode lines per data segment (24) and flip angle (20°) were as for the phantom acquisitions and as for the subsequent in vivo acquisitions. The simulations were repeated with the dynamic-TI algorithm incorporated. The sequence repeat time intervals used in the simulation study were those from an example patient study (image data in Figure 5).

Patient studies

The patient population consisted of 17 consecutive patients (mean age 65.4 years, range 50 – 77 years, 5 female) undergoing 3D LGE imaging prior to RF ablation of symptomatic drug-refractory long-standing persistent AF, as defined by 2012 international guidelines (23). These patients were, by definition, in non-sinus rhythm. All were treated with warfarin to reduce their thromboembolic risk and with rate control drugs. All patients gave written informed consent according to the requirements of the local ethics committee and all data were acquired on a Siemens Avanto 1.5 Tesla scanner (Siemens Medical Systems, Erlangen, Germany).

In each patient, imaging was performed both with and without the dynamic-TI algorithm, the order of acquisitions being randomised to avoid bias. Imaging was started 15 minutes after gadolinium administration (Gadovist - gadobutrol, 0.1mmol/kg body weight in accordance with the manufacturer's guidelines). A conventional 2D breath-hold LGE acquisition was performed with alternate R-wave gating, or for very fast heart rates, with gating on every 3^{rd} or 4^{th} cardiac cycle, in a mid short axis plane to determine the inversion time (TI_{ref}) required to null normal myocardium. (In practice, this also depended on breath-holding capability.) The initial estimate of the TI required to null myocardium was 280 ms.

This was then modified, based on the image appearance, and the breath-hold acquisition repeated until the reference myocardial TI (TI_{ref}) was determined as that TI which resulted in the best myocardial nulling. This typically required 3 - 4 breath-hold acquisitions. While an inversion recovery cine scout acquisition could potentially have been used instead, this is not the method of preference at our institution. The reference myocardial T1 ($T1_{myo}$) was initially estimated from this TI_{ref} ($T1_{myo} = 0.693 \times TI_{ref}$). This estimate was then iteratively adjusted in steps of 5 ms until the calculated TI for this sequence repeat time interval (determined from equation (1)) was equal to that measured. Transverse navigator gated 3D LGE imaging (32 – 36 slices 4mm slices, reconstructed to 64 – 72 slices 2mm slices) was then performed with an end-expiratory following crossed-pairs navigator positioned over the dome of the right hemi-diaphragm with nominal navigator acceptance window size of 6 mm. A chemical-shift fat suppression pre-pulse was used and the acquisition window of 125 ms was positioned in the subject-specific diastolic rest period. All other parameters were as for the phantom acquisition. Nominal acquisition durations were 178 - 242 cardiac cycles, assuming 100% respiratory efficiency. The TI_{ref} and the time between sequence repeats for the TI_{ref} acquisition were included in the sequence parameter list to enable the calculation of $T1_{myo}$ (as described above) which was necessary for the calculation of TI for single R-wave gating, both with and without the dynamic-TI algorithm. The 3D LGE acquisition was performed both with and without the dynamic-TI algorithm with the TI_{ref} being updated prior to the second study to account for gadolinium wash-out.

Analysis and statistics—All statistical tests were performed using IBM SPSS Statistics 19 Package. (1) Image quality score: All 3D LGE datasets (with and without dynamic-TI) were presented to two experienced observers who were blinded to the patient and to the inclusion or not of the dynamic-TI algorithm. Datasets were graded on a 4 point scale (0 = non-diagnostic, moderate – severe ghosting, with or without poor myocardial nulling; 1 = poor, moderate ghosting, with or without poor myocardial nulling, 2 = fair, minor ghosting with good myocardial nulling; 3 = good, minimal ghosting with good myocardial nulling) and in cases of disagreement, a consensus score achieved. Image quality scores with and without dynamic-TI were compared with a paired Wilcoxon test. (2) In each acquisition in each patient, the blood signal-to-ghosting ratio (SGR) was determined as the average ratio of the atrial blood pool signal intensity to the standard deviation of the signal intensity in a region of free space adjacent to the chest wall. The free space region of interest was positioned just to the left or right of the chest cavity (anterior to the arms) and included ghosting artefact in the left-right phase encoding direction due to variable longitudinal magnetisation recovery between sequence repeats. Blood SGR values with and without the dynamic-TI were compared with a paired t-test (after checking for normality). While this may not be strictly speaking the most appropriate method for acquisitions using GRAPPA (24), it is reasonable in this study where paired comparisons are being made. Myocardial SGR was measured in a similar way. In addition blood-myocardium contrast-to-ghosting ratios (CGRs) were determined as the difference in the blood pool and myocardium intensities divided by the standard deviation of the intensity of the same free space region of interest as above, therefore again including ghosting artefact. The CGR values with and without the dynamic-TI algorithm were compared with a paired t-test (after checking for normality). A measure of ghosting was also determined as the ratio of the mean signal

intensity in the region of free space which included ghosting artefact (as defined above) to the standard deviation of the signal intensity in a region of free space anterior to the chest wall. Ghosting ratios with and without dynamic-TI were compared with a Wilcoxon matched-pairs. For all analyses, a p value < .05 was considered to be statistically significant.

Results

Phantom studies

Figure 2 shows the results of the phantom study. In (a), acquired with a sequence repeat time interval of 2000 ms and an inversion time of 325 ms (TI_{ref}), the bottle representing normal myocardium (top) is nulled. In (b), the sequence repeat time interval is reduced to 1000 ms and the TI calculated by equation (1) (275 ms) results in good nulling of the simulated myocardium. In (c) and (d), acquisitions were performed with the simulated RR interval varying randomly from 700 – 1300 ms, with and without the dynamic-TI algorithm respectively. In (c), variations in the longitudinal magnetisation recovery between sequence repeats have resulted in ghosting which is reduced in (d). The sequence repeat time interval variabilities (expressed as the standard deviation as a percentage of the mean) for these acquisitions were 13.1% and 12.0% respectively. In (e) and (f), the acquisitions in (c) and (d) were repeated with frequent missed cardiac triggers (resulting in sequence repeat time variabilities 31.4% and 30.5% respectively). Without the dynamic-TI algorithm (e), the ghosting due to variable longitudinal magnetisation recovery is increased and the fixed TI (calculated for an RR interval of 1000 ms) is incorrect. The dynamic-TI algorithm increased the mean simulated blood-myocardium CGR from 12.1 to 21.8 for the acquisition without missed cardiac triggers ((c) and (d)), and from 0.8 to 20.6 for the acquisition with missed cardiac triggers ((e) and (f)). The corresponding mean simulated enhanced tissue-myocardium CGR values increased from 55.3 to 98.3 ((c) and (d)) and from 30.1 to 91.1 ((e) and (f)) respectively.

Simulation study

The efficacy of the dynamic-TI algorithm is demonstrated in the simulation of Figure 3 which shows the % longitudinal magnetisation, M_z, of blood (estimated T1 = 420ms), myocardium (estimated T1 = 490ms) and shorter T1 tissue (360 ms) for the most central k-space line in each data segment of an inversion prepared segmented gradient echo acquisition with single R-wave gating without (left) and with (right) the dynamic-TI algorithm in a subject with heart rate variability. The simulation is shown over 16 cardiac cycles - the first two being dummies - for repeat time intervals ranging from 633 – 1433 (mean 923 +/− 256 ms). Implementation of the dynamic-TI algorithm reduces the variations in M_z at the centre of k-space for myocardium from 3.6 +/− 8.4 to 2.0 +/− 0.9 and for blood from 9.6 +/− 7.3 to 7.9 +/− 0.7. For the shorter T1 tissue, M_z variations are reduced from 16.7 +/− 6.0 to 14.8 +/− 2.3.

Patient Studies

3D LGE acquisitions with and without dynamic-TI were completed in all 17 patients, the acquisition duration being 452 +/− 148 cardiac cycles. There was no significant difference between the acquisition times with and without the dynamic-TI algorithm (456 +/− 158 s vs

448 +/− 140 s, p = ns). The sequence repeat time intervals stored with each acquisition show the time between sequence repeats which varies due to a combination of changes in the RR intervals and missed cardiac triggers which may be frequent in fast AF. Paired analysis of the sequence repeat time intervals stored with the two sets of data showed that there were no significant differences between the mean values in the acquisitions with and without dynamic-TI (913.4ms +/− 67.9ms vs 909.8ms +/− 71.3 ms respectively, p = ns). There was also no significant difference between the sequence repeat time interval variability (expressed as the standard deviation of the sequence repeat time intervals as a percentage of the mean) with and without dynamic-TI (26.3% +/− 6.4%, (range 17.4% - 44.3%) vs 25.5% +/− 5.6%, (range 17.3% - 34.1%) respectively, p = ns).

For acquisitions both with and without dynamic-TI, the sequence repeat time variability in subjects having a fair or good image quality (score 2 or 3) was significantly lower than that in subjects with a non-diagnostic or poor image quality (score 0 or 1) (with dynamic-TI: 24.0% +/− 4.6% vs 31.8% +/− 7.1% respectively, p = .015; without dynamic-TI: 23.1% +/− 5.6% vs 29.8% +/− 1.6% respectively, p = .012). On average, the consensus image quality scores were higher in acquisitions with the dynamic-TI algorithm compared to those without (2.2 +/− 0.9 vs 1.8 +/− 1.1, p = 0.008). In 8 subjects (47%), the dynamic-TI algorithm improved the consensus image quality score, in 8 subjects (47%), the consensus image quality score was unchanged and in 1 subject (6%), it decreased. In this last subject, the percentage sequence repeat time variability was much higher in the acquisition with dynamic-TI (44.3%) than it was in the acquisition without dynamic-TI (34.1%). The subjects showing an improvement with the dynamic-TI algorithm had a higher percentage sequence repeat time variability than those showing no improvement, although this did not reach statistical significance (27.2% +/− 2.8% vs 23.1% +/− 5.2%, p = 0.07).

The dynamic-TI algorithm improved blood pool SGR (19.6 +/− 8.5 vs 13.1 +/− 8.0, p = 0.003). Similarly, the dynamic-TI algorithm resulted in a statistically significant improvement in blood-myocardium CGR (13.81 +/− 7.56 vs 8.32 +/− 6.06, p = 0.003). As would be expected, both the blood SGR and the blood-myocardium CGR were strongly related to the subjective image quality score (blood SGR: 10.2 +/− 6.3 vs 19.3 +/− 8.4 for image quality scores 0/1 and 2/3 respectively, p = 0.003 and CGR: 6.2 +/− 5.6 vs 13.4 +/− 6.9 for image quality scores 0/1 and 2/3 respectively, p = 0.005). Patients with a subjective improvement in image quality with the dynamic-TI algorithm had a greater improvement in the blood pool SGR (11.0 +/− 6.5 vs 2.5 +/− 6.2, p = .015) and blood-myocardium CGR (9.2 +/− 7.0 vs 2.2 +/− 3.3, p = .015) than those without subjective improvement. There was no significant difference in the myocardial SGR with and without the dynamic-TI algorithm (4.6 +/− 2.0 vs 4.0 +/− 2.7, p = ns). The dynamic-TI algorithm resulted in images with a significantly reduced and less variable ghosting ratio (10.8 +/− 4.3 vs 15.8 +/− 8.7, p = 0.004).The image quality scores, blood-myocardium SGRs and blood-myocardium CGRs for low (<22.5%), medium (22.5 – 30%) and high (>30%) sequence repeat time interval variability are summarised in Figure 4 for acquisitions both with and without the dynamic-TI algorithm.

Figures 5 and 6 show example patient acquisitions with and without the dynamic-TI algorithm demonstrating reduced ghosting and improved image quality with the dynamic-TI

algorithm. Figure 6 shows an example where, in addition to ghosting, the acquisition without dynamic-TI shows incorrect signal nulling. The corresponding sequence repeat time variability histograms for these subjects are also shown. The high percentage of missed cardiac triggers in the patient in Figure 6 (which result in frequent extended sequence repeat time intervals and a dominant second peak) is most likely responsible for the poor signal nulling. For all patients, the with and without dynamic-TI distributions of sequence repeat time intervals are similar.

Discussion

We have implemented a dynamic-TI inversion scheme and have shown that it results in improved 3D LGE image quality in patients with persistent AF. The algorithm results in increased blood signal-to-ghosting ratios and increased blood-myocardium contrast-to-ghosting ratios. Myocardial SGR is unchanged. In nearly half of the patients (47%), there was also a small but significant increase in the consensus image quality score. The improvement in image quality score was greatest in those subjects having the highest degree of sequence repeat time variation.

Poor image quality is a frequent cause of concern in AF patients (18). However, while other studies have reported that the percentage of non-diagnostic scans ranging from 15% (14) to 41% (10), the percentage of patients with poor quality data who were in non sinus rhythm at the time of those scans has not reported. The extent of this problem is therefore unclear although in our study of patients with persistent AF, non-diagnostic or poor image quality was observed in 6 (35%) of 17 patients. This was due to a combination of RR interval variability and missed cardiac triggers, as shown in the lower panel in Figure 6. However, the image appearance will depend not only on the shape of these sequence repeat time histograms, but also on the timing of any variability relative to the k-space data being acquired. This will be a focus of further work. As seen in Figure 6, the missed cardiac triggers result in non-normal distributions of the sequence repeat time variability. Consequently, characterising the repeat time interval variability as the standard deviation as a percentage of the mean is limited. In our subject group, 24 hour holter monitoring was not conducted prior to ablation so we could compare the cardiac rhythm of our subjects with typical AF traces.

As demonstrated in Figure 3, the algorithm implemented aims to reduce variations in the longitudinal magnetisation of myocardium throughout the acquisition, regardless of the sequence repeat time interval. While longitudinal magnetisation variation of other tissues (blood, enhanced tissue) remains, it is reduced in amplitude, as shown in Figure 3(b), and image quality is improved, as shown in Figures 2(d) and (f). However, the technique is not capable of removing the Mz variations from all of the tissues all of the time. Further work will investigate the effects of minimising Mz of different tissues on image quality but this is beyond the scope of this current manuscript. While the dynamic-TI technique succeeds in reducing the longitudinal magnetisation variation throughout the acquisition, further improvements may be made by rejecting and reacquiring views acquired in extreme sequence repeat time intervals, which may be due to either arrhythmia or to missed cardiac triggers. Not only would this further reduce the longitudinal magnetisation variation

throughout the acquisition, but it would also be necessary to ensure consistency of the heart position and filling from one repeat interval to the next and to reduce the resulting cardiac blurring..

With this sequence, inputting the reference myocardial TI (TI_{ref}) and the sequence repeat time interval for this reference acquisition can be used to estimate the TI at a fixed, as well as at a variable, sequence repeat time interval. This is in fact an option on the user interface – if dynamic-TI is not used (tickbox unchecked), the user can enter a target sequence repeat time interval for which the TI is to be calculated and the subsequent acquisition (without dynamic-TI) is run. An example of the efficacy of this is provided in Figures 2 (a) and (b) where the image in (a) is acquired with the same sequence repeat time interval as the scout (2000 ms) and TI = TI_{ref} ie the TI required to null nomal myocardium at this sequence repeat time interval, while in (b) the target sequence repeat time interval is 1000 ms and the TI has been calculated accordingly. The efficacy of the calculation is supported by the phantom acquisitions in (b) and the dynamic-TI acquisitions in (d) and (f). Based on equation (1), we have previously created look up tables of TI (for single R-wave gating) versus sequence repeat time interval for a range of TI_{ref} (25). However, embedding the calculation of TI within the sequence code, as done here, is easier as it avoids the need for these tables.

The estimate of the myocardial T1 ($T1_{myo}$ in equation (1)) requires the user to input the estimated inversion time to null normal myocardium (TI_{ref}) and the time between sequence repeats for this estimate of TI_{ref} (2 – 4 × RR intervals, depending on base heart rate). The latter is currently determined from visual display of the patient's ECG. However, a less subjective alternative would be to record the sequence repeat time intervals throughout the reference TI acquisition and to determine an average. This will be implemented in future work. Sequence repeat time interval variations will affect the accuracy of TI_{ref}. However, if the repeat time intervals for the reference acquisition are sufficiently long (2 – 4 RR intervals), almost complete longitudinal magnetization recovery will occur between sequence repeats and the effects of RR interval variability will be minimized. Errors in the estimation of $T1_{myo}$ and of the TI for the single R-wave gating acquisitions will therefore also minimized.

For this study, the contrast agent dose was .1mmol per kg (gadobutrol) as suggested by the manufacturer (Gadovist). While this is the standard dose used in our institution, it is lower than that used with some other gadolinium-based contrast agents in other institutions. Higher doses will lead to differences in TI_{ref} and $T1_{myo}$ and may change the efficacy of the dynamic-TI algorithm. This will be the subject of further work.

To our knowledge, this study shows the first application of this technique in patients with AF and it shows that dynamic adaptation of the inversion time on a beat by beat basis results in reduced longitudinal magnetisation variation throughout the acquisition and that qualitative and quantitative measures of image quality are improved.

In conclusion, dynamic adaptation of the inversion time from beat-to-beat significantly improves subjective image quality and significantly improves blood pool signal-to-ghosting

ratios and blood-myocardium contrast-to-ghosting ratios in patients with AF. This improved image quality will assist automatic atrial LGE quantification in the atria in this difficult patient population.

Acknowledgement

Sonya V. Babu-Narayan is supported by an Intermediate Clinical Research Fellowship from the British Heart Foundation. This project was supported by Wellcome Trust Grant WT093953MA and the NIHR Cardiovascular Biomedical Research Unit of Royal Brompton and Harefield NHS Foundation Trust and Imperial College London. This report is independent research by the National Institute for Health Research Biomedical Research Unit Funding Scheme. The views expressed in this publication are those of the author(s) and not necessarily those of the NHS, the National Institute for Health Research or the Department of Health.

References

1. Fuster V, Rydén LE, Cannom DS, Crijns HJ, Curtis AB, Ellenbogen KA, Halperin JL, Le Heuzey JY, Kay GN, Lowe JE, Olsson SB, Prystowsky EN, Tamargo JL, Wann S, Smith SC Jr, Jacobs AK, Adams CD, Anderson JL, Antman EM, Halperin JL, Hunt SA, Nishimura R, Ornato JP, Page RL, Riegel B, Priori SG, Blanc JJ, Budaj A, Camm AJ, Dean V, Deckers JW, Despres C, Dickstein K, Lekakis J, McGregor K, Metra M, Morais J, Osterspey A, Tamargo JL, Zamorano JL. ACC/AHA/ESC 2006 Guidelines for the Management of Patients with Atrial Fibrillation: a report of the American College of Cardiology/American Heart Association Task Force on Practice Guidelines and the European Society of Cardiology Committee for Practice Guidelines: developed in collaboration with the European Heart Rhythm Association and the Heart Rhythm Society. Circulation. 114:e257–354. [PubMed: 16908781]
2. Oral H, Knight B, Ozaydin M, Chugh A, Lai S, Scharf C, Hassan S, Greenstein R, Han J, Pelosi F, Strickberger A, Morady F. Segmental ostial ablation to isolate the pulmonary veins during atrial fibrillation: feasibility and mechanistic insights. Circulation. 2002; 106:1256–1262. [PubMed: 12208802]
3. Haissaguerre M, Jais P, Shah DC, Takahashi A, Hocini M, Quiniou G, Garrigue S, Le Mouroux A, Le Metayer P, Clementy J. Spontaneous initiation of atrial fibrillation by ectopic beats originating in the pulmonary veins. N Engl J Med. 1998; 339:659–666. [PubMed: 9725923]
4. Ganesan AN, Shipp NJ, Brooks AG, Kuklik P, Lau DH, Lim HS, et al. Long-term outcomes of catheter ablation of atrial fibrillation: a systematic review and meta-analysis. J Am Heart Assoc. 2013; 2:e004549. [PubMed: 23537812]
5. Peters D, Wylie J, Hauser T, Kissinger K, Botnar R, Essebag V, Josephson M, Manning W. Detection of pulmonary vein and left atrial scar after catheter ablation with three-dimensional navigator-gated delayed enhancement MR imaging. Radiology. 2007; 243:690–695. [PubMed: 17517928]
6. Wylie JV Jr, Peters DC, Essebag V, Manning WJ, Josephson ME, Hauser TH. Left atrial function and scar after catheter ablation of atrial fibrillation. Heart Rhythm. 2008; 5:656–662. [PubMed: 18452866]
7. Oakes RS, Badger TJ, Kholmovski EG, Akoum N, Burgon NS, Fish EN, Blauer JJ, Rao SN, DiBella EV, Segerson NM, Daccarett M, Windfelder J, McGann CJ, Parker D, MacLeod RS, Marrouche NF. Detection and quantification of left atrial structural remodelling with delayed-enhancement magnetic resonance imaging in patients with atrial fibrillation. Circulation. 2009; 119:1758–1767. [PubMed: 19307477]
8. McGann CJ, Kholmovski EG, Oakes RS, Blauer JJ, Daccarett M, Segerson N, Airey KJ, Akoum N, Fish E, Badger TJ, DiBella EV, Parker D, MacLeod RS, Marrouche NF. New magnetic resonance imaging-based method for defining the extent of atrial wall injury after the ablation of atrial fibrillation. J Am Coll Cardiol. 2008; 52:1263–1271. [PubMed: 18926331]
9. Badger T, Oakes R, Daccarett M, Burgon N, Akoum N, Fish E, Blauer J, Rao S, Adjei-Poku Y, Kholmovski E, Vijayakumar S, Di Bella E, MacLeod R, Marrouche N. Temporal left atrial lesion formation after ablation of atrial fibrillation. Heart Rhythm. 2009; 6:161–168. [PubMed: 19187904]

Europe PMC Funders Author Manuscripts

10. Peters D, Wylie J, Hauser T, Nezafat R, Han Y, Woo J, Taclas J, Kissinger K, Goddu B, Josephson M, Manning W. Recurrence of atrial fibrillation correlates with the extent of post-procedural late gadolinium enhancement: a pilot study. J Am Coll Cardiol Imag. 2009; 2:308–316.
11. Badger T, Daccarett M, Akoum N, Adjei-Pou Y, Burgon N, Haslam T, Kalvaitis S, Kuppahally S, Vergara G, McMullen L, Anderson P, Kholmovski E, MacLeod R, Marrouche N. Evaluation of left atrial lesions after initial and repeat atrial fibrillation ablation: lessons learned from delayed-enhancement MRI in repeat ablation procedures. Circ Arrhyth Electrophysiol. 2010; 3:249–259.
12. Daccarett M, Badger TJ, Akoum N, Burgon N, Mahnkopf C, Vergara G, Kholmovski E, McGann C, Parker D, Brachmann J, MacLeod R, Marrouche N. Association of left atrial fibrosis detected by delayed enhancement magnetic resonance imaging and the risk of stroke in patients with atrial fibrillation. J Am Coll Cardiol. 2011; 57:831–8. [PubMed: 21310320]
13. Akoum N, McGann C, Vergara G, Badger T, Ranjan R, Mahnkopf C, Kholmovski E, MacLeod R, Marrouche N. Atrial fibrosis quantified using late gadolinium enhancement MRI is associated with sinus node dysfunction requiring pacemaker implant. J Cardiovasc Electrophysiol. 2012; 23:44–50. [PubMed: 21806700]
14. Akoum M, Daccarett M, McGann C, Segerson N, Vergara G, Kuppahally S, Badger T, Burgon N, Haslam T, Kholmovski E, MacLeod R, Marrouche N. Atrial fibrosis helps select the appropriate patient and strategy in catheter ablation of atrial fibrillation: A DE-MRI guided approach. J Cardiovasc Electrophysiol. 2011; 22:16–22. [PubMed: 20807271]
15. Daccarett M, McGann C, Akoum N, MacLeod R, Marrouche N. MRI of the left atrium: predicting clinical outcomes in patients with atrial fibrillation. Expert Rev Cardiovasc Ther. 2011; 9:105–111. [PubMed: 21166532]
16. Vergara GR, Marrouche NF. Tailored management of atrial fibrillation using a LGE-MRI based model: from the clinic to the electrophysiology laboratory. J Cardiovasc Electrophysiol. 2011; 22:481–487. [PubMed: 21044212]
17. Kellman P, Arai AE. Cardiac imaging techniques for physicians: late enhancement. J Magn Reson Imaging. 2012; 36:529–542. [PubMed: 22903654]
18. Knowles B, Caulfield D, Cooklin M, Rinaldi A, Gill J, Bostock J, Razavi R, Schaeffter T, Rhode K. 3-D visualization of acute RF ablation lesions using MRI for the simultaneous determination of the patterns of necrosis and edema. IEEE Trans Biomedical Engineering. 2010; 57:1467–1475.
19. Weingartner S, Akcakaya M, Basha T, Kissinger K, Goddu B, Berg S, Manning W, Nezafat R. Combined saturation/inversion recovery sequences for improved evaluation of scar and diffuse fibrosis in patients with arrhythmia or heart rate variability. Magn Reson Med. 2013 doi: 10.1002/mrm.24761.
20. He T, Gatehouse P, Anderson L, Tanner M, Keegan J, Pennell D, Firmin D. Development of a novel optimised breath-hold technique for myocardial T2 measurement of thalassemia. J Magn Reson Imaging. 2006; 24:580–585. [PubMed: 16892203]
21. Fleckenstein JL, Archer BT, Barker BA, Vaughn JT, Parkey RW, Peshock RM. Fast short-tau inversion recovery MR imaging. Radiology. 1991; 179:499–504. [PubMed: 2014300]
22. Griswold M, Jakob PM, Heidermann RM, Nittka M, Jellus V, Wang J, Kiefer B, Haase A. Generalized autocalibrating partially parallel acquisitions (GRAPPA). Magn Reson Med. 2002; 47:1202–1210. [PubMed: 12111967]
23. Calkins H, Kuck KH, Cappato R, et al. 2012 HRS/EHRA/ECAS expert consensus statement on catheter and surgical ablation of atrial fibrillation: recommendations for patient selection, procedural techniques, patient management and follow-up, definitions, endpoints, and research trial design. Europace. 2012; 14:528–606. [PubMed: 22389422]
24. Kellman P, McVeigh ER. Image reconstruction in SNR units: a general method for SNR measurement. Magn Reson Med. 2005; 54:1439–1447. [PubMed: 16261576]
25. Keegan J, Jhooti P, Babu-Narayan SV, Drivas P, Ernst S, Firmin D. Improved respiratory efficiency of 3D late gadolinium enhancement imaging using the continuously adaptive windowing strategy (CLAWS). Magn Reson Med. 2013 doi: 10.1002/mrm.24758.

Europe PMC Funders Author Manuscripts

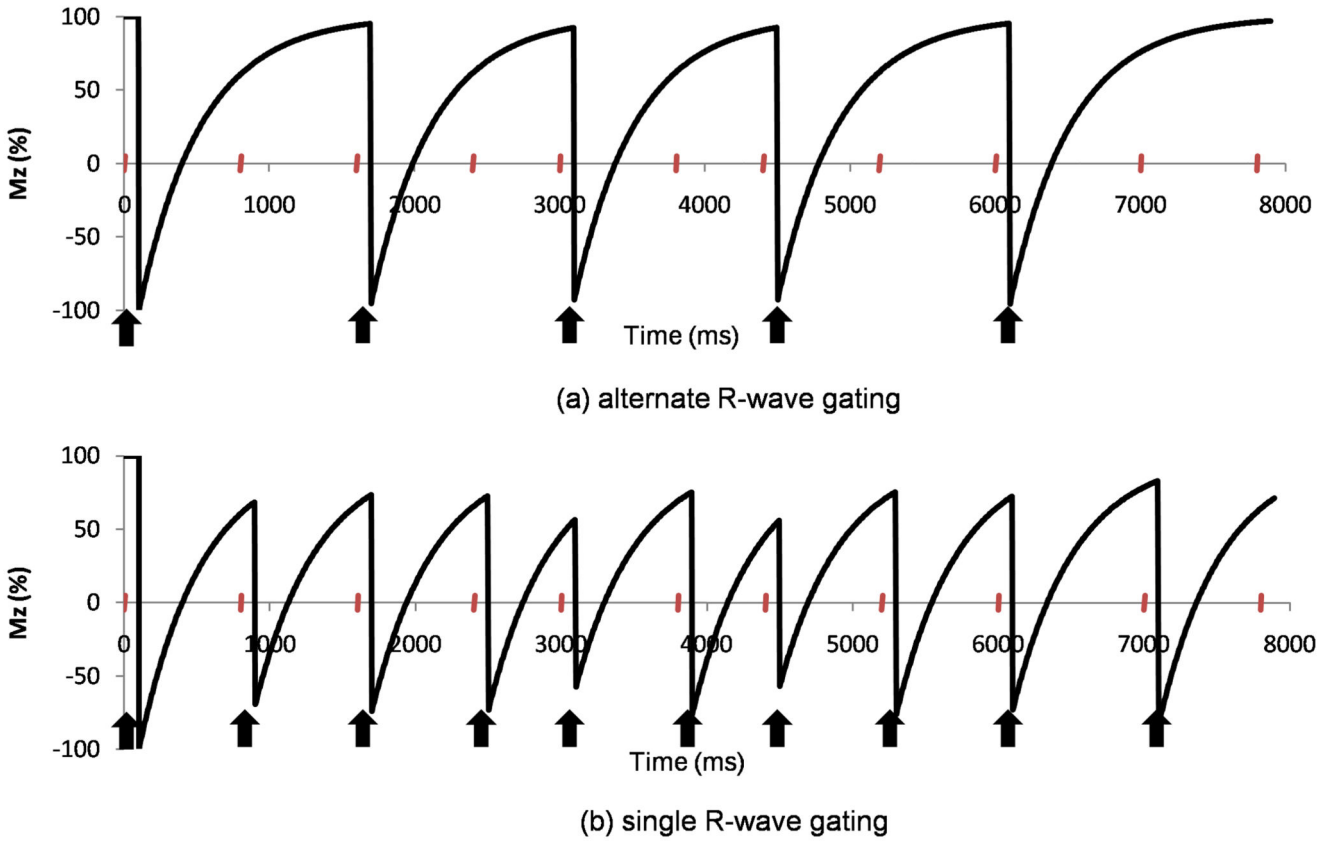

Figure 1.

Simulated longitudinal magnetisation, M_z (as a percentage of the initial longitudinal magnetization, M_0), following inversion preparation over 10 cardiac cycles with variable RR intervals: (a) with alternate R-wave gating and (b) with single R-wave gating. The curves are simulated for a T1 of 430ms and the simulated RR intervals are 800ms, 800ms, 800ms, 600ms, 800ms, 600ms, 800ms, 800ms, 1000ms, 800ms. The timing of the R-waves is marked with ticks on the time axis and the inversion pulses are marked by arrows. (The effect of the LGE readout is small for short T1 and low flip angle and has been ignored in these simulations.)

Europe PMC Funders Author Manuscripts

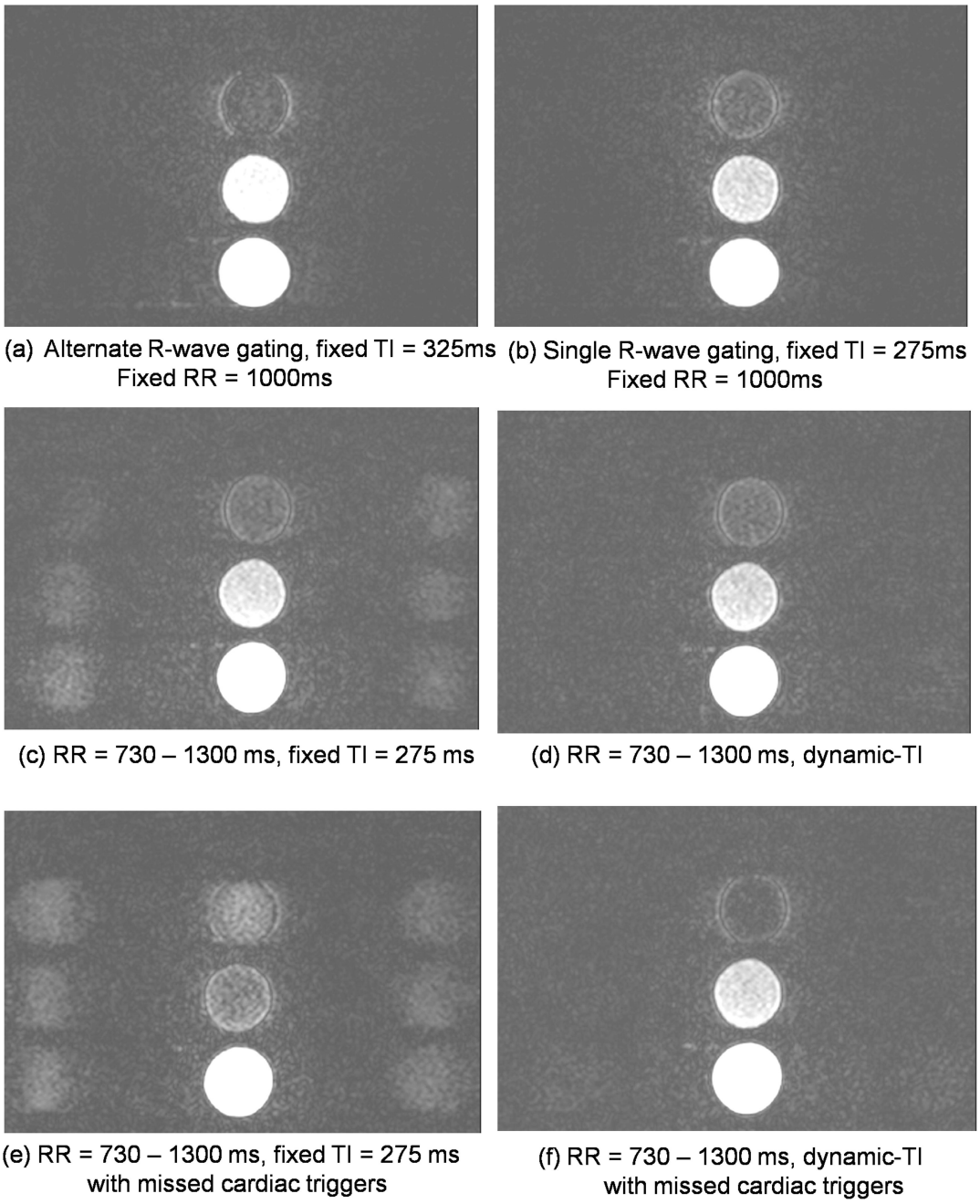

Figure 2.

Phantom acquisitions with and without dynamic-TI. The phantom consists of three bottles having T1s of 490 ms (simulated myocardium (top)), 420 ms (simulated blood (middle)) and 360 ms (simulated shorter T1 tissue (bottom)). Example images acquired with (a) sequence repeat time interval 2000 ms and TI_{ref} of 325 ms to null simulated myocardium, (b) sequence repeat time interval 1000 ms and TI calculated from equation 1 (275 ms), (c) sequence repeat time intervals varying randomly from 700 – 1300 ms (without dynamic-TI), using the TI determined for a target sequence repeat time interval of 1000 ms as in (b) (ie TI

= 275 ms). The standard deviation of the sequence repeat time intervals (as a percentage of the mean) was 13.1%. Simulated blood-myocardium CGR = 12.1, simulated enhanced tissue-myocardium CGR = 55.3. (d) simulated RR interval varying randomly between 700 ms and 1300 ms using a TI determined on a beat by beat basis by equation (1). The standard deviation of the sequence repeat time intervals (as a percentage of the mean) was 12.0%. Simulated blood-myocardium CGR = 21.8, simulated enhanced tissue-myocardium CGR = 98.3. (e) simulated RR interval varying randomly between 700 ms and 1300 ms (without dynamic-TI), using the TI determined for a target sequence repeat time interval of 1000 ms as in (b) above (TI = 275 ms). In this acquisition, frequent missed cardiac triggers resulted in the sequence repeat time intervals varying from 819 – 2031 ms with the standard deviation (as a percentage of the mean) being 31.4%. Simulated blood-myocardium CGR = 0.8, simulated enhanced tissue-myocardium CGR = 30.1. (f) simulated RR interval varying randomly between 700 ms and 1300 ms, using a TI being determined on a beat by beat basis by equation (1). In this acquisition, frequent missed cardiac triggers resulted in the sequence repeat time intervals varying from 795 – 2007 ms with the standard deviation (as a percentage of the mean) being 30.5%.

Europe PMC Funders Author Manuscripts

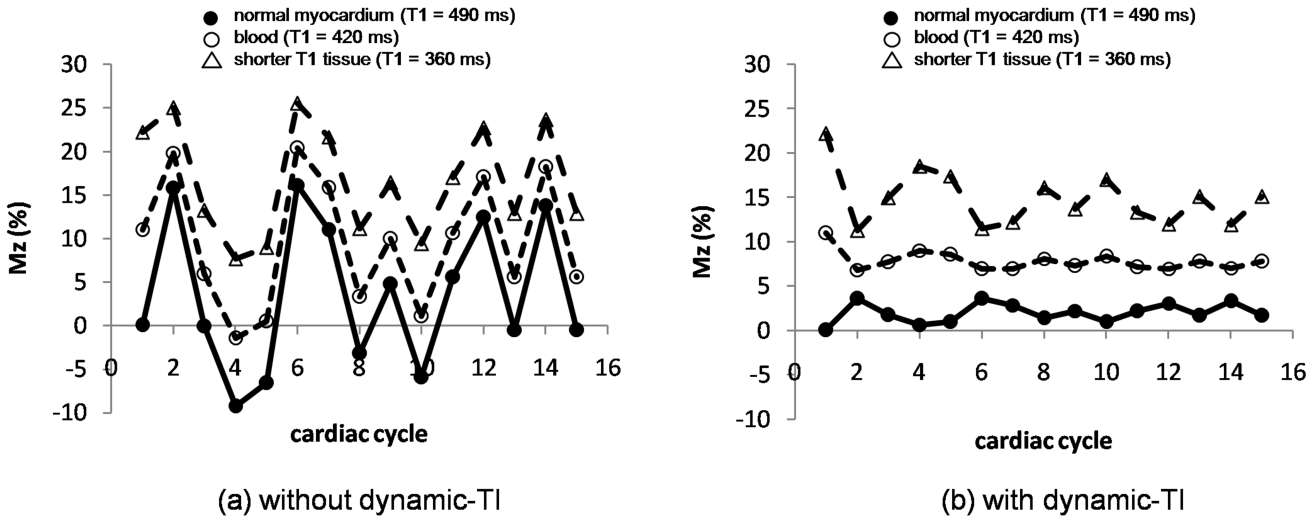

Figure 3.

Longitudinal magnetization, M_z (as a percentage of the initial longitudinal magnetization, M_0) of blood (open circles, T1 = 420 ms) and myocardium (filled circles, T1 = 490 ms) for the most central k-space line in an inversion prepared segmented gradient echo acquisition with single R-wave gating without (left) and with (right) dynamic-TI in a subject with variable heart rate. A shorter T1 tissue is also simulated (open triangles, T1 = 360 ms). The sequence repeat time intervals were from an example patient (Figure 4): 633ms, 966ms, 1433ms, 1266ms, 633ms, 699ms, 1083ms, 850ms, 1216ms, 833ms, 683ms, 983ms, 666ms, 983ms. The first two cardiac cycles were dummy cycles. The longitudinal magnetization at the centre of k-space is less variable for all T1s with the dynamic-TI algorithm.

Europe PMC Funders Author Manuscripts

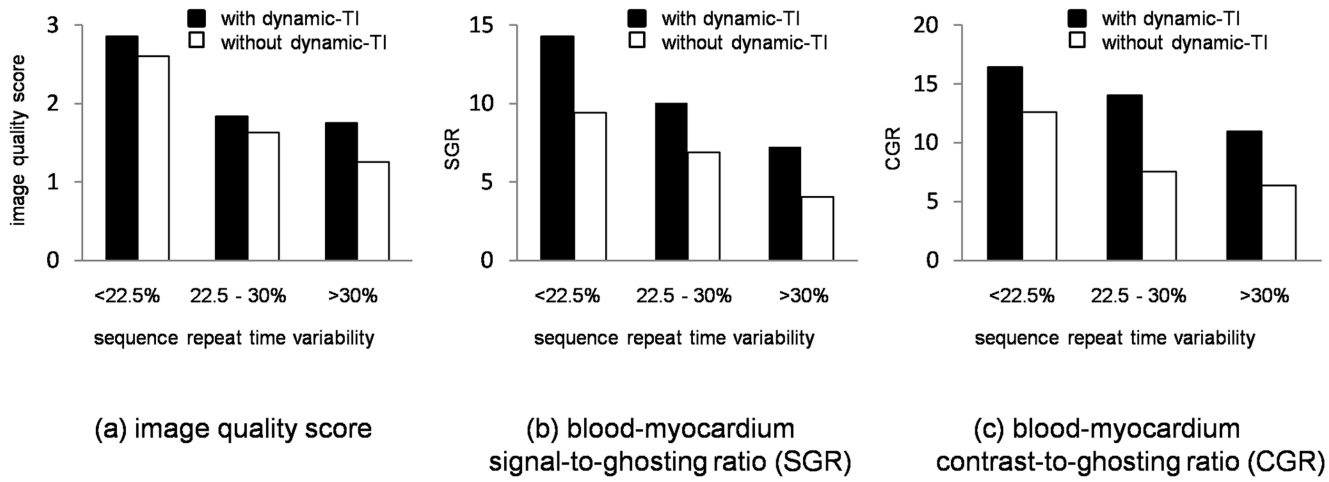

Figure 4.

Mean image quality scores (a), blood-myocardium SGRs (b) and blood-myocardium CGRs (c) as a function of sequence repeat time interval variability (standard deviation as a percentage of the mean) for acquisitions with and without the dynamic-TI algorithm.

Europe PMC Funders Author Manuscripts

Europe PMC Funders Author Manuscripts

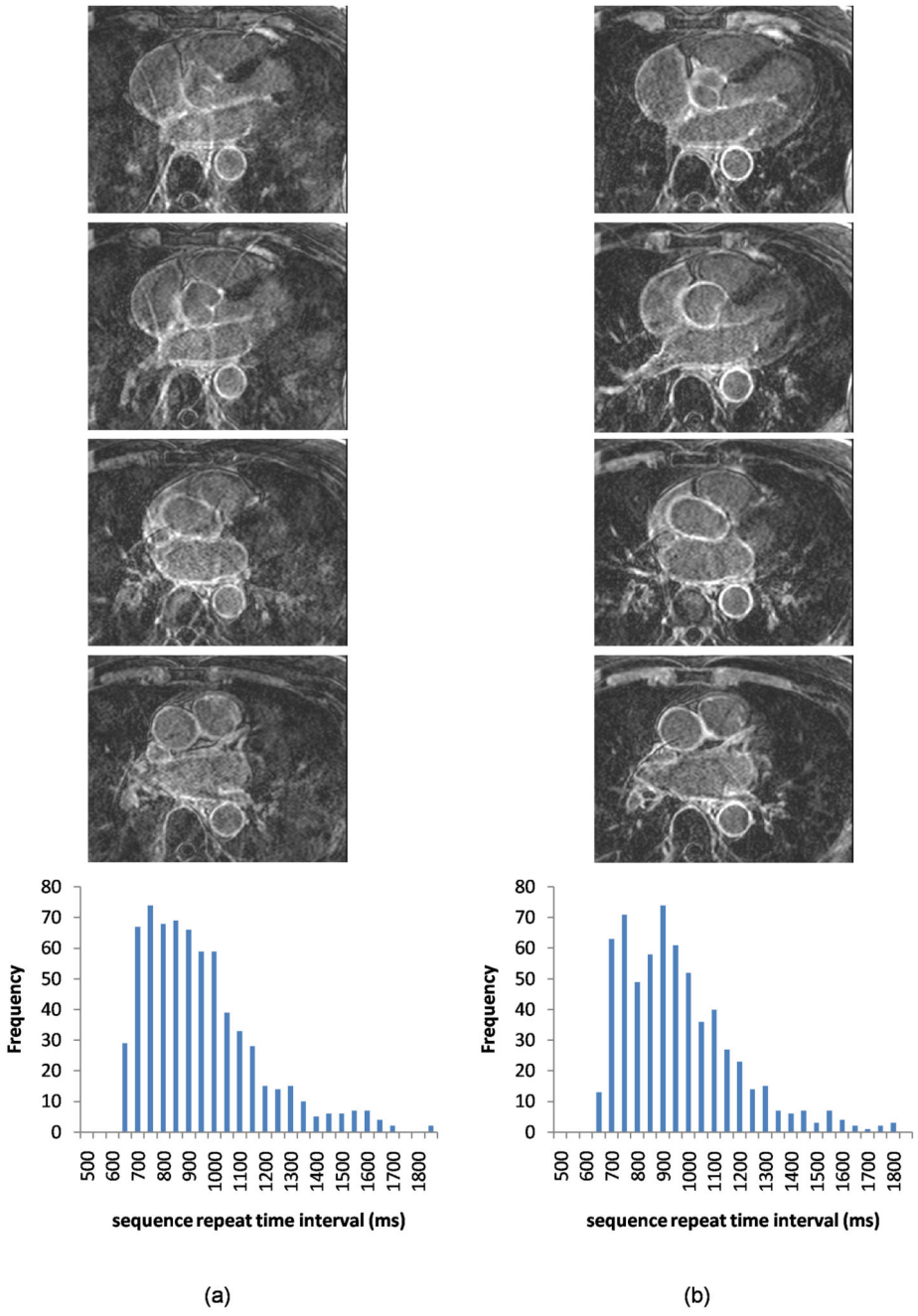

Figure 5.

Selected slices from 3D acquisitions in an example patient both without (a) and with (b) dynamic-TI, together with sequence repeat time interval histograms. The dynamic-TI algorithm results in less ghosting in the left-right phase encode direction and improved image quality. The image quality score increased from 2 to 3 with the dynamic-TI algorithm. The window width and level have been set to best demonstrate the artefact levels in the images. The repeat time intervals were similar in the acquisitions with and without dynamic-TI (standard deviation as a percentage of the mean 25.1% and 24.8% respectively).

Europe PMC Funders Author Manuscripts

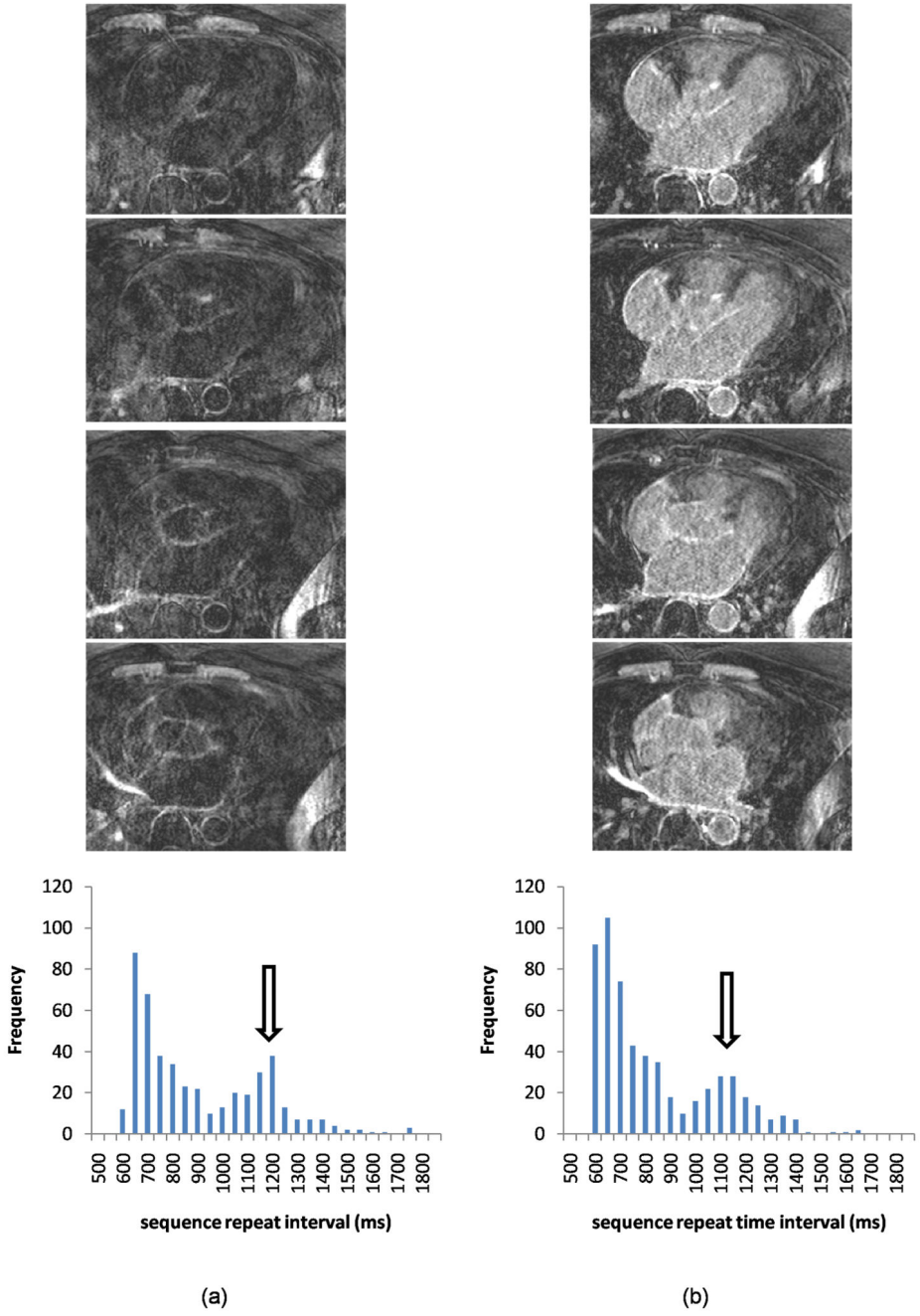

Figure 6.

Selected slices from 3D acquisitions in an example patient both without (a) and with (b) dynamic-TI, together with sequence repeat time interval histograms. In this subject, there were frequent missed cardiac triggers resulting in frequent extended sequence repeat time intervals (open arrows) which without dynamic-TI, result in incorrect signal nulling and ghosting (image quality score 0). Image quality is improved with dynamic-TI (image quality score 1). The image quality score increased from 0 to 1 with the dynamic-TI algorithm. The window width and level have been set to best demonstrate the artefact levels in the images.

The repeat time intervals were similar in the acquisitions with and without dynamic-TI (standard deviation as a percentage of the mean 28.4% and 29.4% respectively).

Europe PMC Funders Author Manuscripts